A scalable optimization framework for the design and operation of distributed multi-energy systems

Amirmohammad Khojastefar[a], Enrico Dal Cin[a], Sergio Rech[a] and Gianluca Carraro[a]

[a] *University of Padova, Industrial Engineering Department, Padova, Italy,*

amirmohammad.khojastefar@studenti.unipd.it

enrico.dalcin@phd.unipd.it

sergio.rech@unipd.it

gianluca.carraro@unipd.it, CA

Abstract:

The success of a comprehensive, integrated design and operation optimization of large-scale Multi-Energy Systems (MESs) is currently hampered by the rapid growth in decision variables and constraints with the extension of the system. To address this limitation, problem decomposition and distributed optimization have emerged as promising solutions. Existing distributed approaches mainly focus on operational coordination or adopt sectorial, stakeholder-based decomposition for integrated electricity–gas planning problems. Spatial decomposition of large-scale MESs remains largely unexplored, especially considering the integrated design and operation of coupled electrical and thermal networks. This work addresses the scalability challenge of large-scale MES optimization by applying spatial decomposition based on the Alternating Direction Method of Multipliers (ADMM), a decomposition–coordination algorithm that splits the full problem into smaller areas coordinated through consensus constraints. The MES is geographically decomposed into interconnected sub-regions, each treated as a local problem, while coordination and consistent power exchanges between areas are ensured by setting proper power flow constraints at the boundaries. The approach is evaluated on a system including coupled electricity and district heating networks. Spatial decomposition is compared with the undecomposed monolithic formulation, used as a benchmark. Results show that decomposing the MES into two areas reduces computational time by 29% with a 0.19% deviation in the objective value compared to the benchmark, while partitioning it into four areas reduces computational time by 65.7% with a 1.6% deviation. This demonstrates that ADMM-based spatial decomposition allows computational load to be drastically reduced without significant accuracy deterioration.

Keywords:

Large Scale Multi-Energy System; Alternating Direction Method of Multipliers; Optimization.

1. Introduction

The European Union has committed to reducing net greenhouse gas emissions by at least 55% by 2030 compared to 1990 levels and to achieving climate neutrality by 2050, while increasing the share of renewable energy to at least 42.5% and reducing final energy consumption by 11.7% [1]. Achieving these objectives requires a shift toward Multi-Energy Systems (MES), as deep decarbonization with high shares of renewables demands coordinated planning and operation of electricity, heat, and other energy carriers to exploit cross-sector flexibility and avoid suboptimal, single-vector solutions [2].

A MES is typically composed of four main subsystems: energy supply, energy conversion, energy transportation, and energy storage. A holistic analysis of MESs therefore requires the simultaneous consideration of all these interacting components. Accordingly, the complete optimization of a MES with respect to a given objective function generally involves three interrelated levels of analysis. The synthesis level determines the system topology, including the number, type, and spatial allocation of energy conversion and storage units needed to satisfy end-user demands. The design level focuses on sizing these units and defining the capacities of the energy networks. Finally, the operation level addresses the optimal dispatch of controllable assets, the management of power and mass flows within the networks, and the implementation of demand response strategies [3]. Optimization problems that jointly address synthesis, design, and operation, commonly referred to as SDO optimization, represent the most comprehensive class of energy system optimization problems, but are also the most challenging to solve due to the large number of coupled continuous and discrete decision variables and constraints [4].

In this context, Dal Cin et al. [5] proposed a new general method based on Mixed Integer Linear Programming (MILP) for the integrated optimization of MESs, with the aim of overcoming the limitations of approaches that

optimize only subsets of MES components while treating the remaining ones as fixed constraints. The proposed formulation enables the simultaneous optimization of energy conversion and storage technologies, energy network capacities, and system operation, while explicitly accounting for life-cycle costs and greenhouse gas emission constraints. This approach proved effective for geographically limited systems, such as urban districts characterized by a relatively small number of nodes. However, when extended to large-scale MESs, for example, city-wide networks, the rapid increase in the number of decision variables and constraints leads to significant computational challenges that limit its practical applicability. Although the model already employs a K-medoids clustering technique to reduce temporal complexity by aggregating time series into representative typical days, further methodological developments are required to enable the scalable optimization of large-scale MESs.

To address the computational complexity associated with large-scale energy system optimization problems, decomposition techniques have been widely investigated in literature. These methods aim to improve tractability by partitioning the original large-scale problem into a set of smaller subproblems that can be solved independently, often in parallel, while coordination is ensured by means of coupling variables and linking constraints that enforce consistency across subproblems [6]. Classical decomposition approaches include Lagrangian relaxation, Benders decomposition, and Dantzig–Wolfe decomposition, which exploit separability across time stages, network components, or decision blocks [7]. In addition, proximal bundle methods, cutting-plane approaches, and augmented Lagrangian techniques have been proposed to improve convergence properties when dealing with non-smooth objectives or complex constraints [8]. Within this class of methods, the Alternating Direction Method of Multipliers (ADMM) has emerged as a particularly effective and widely adopted approach for large-scale distributed optimization. ADMM can be interpreted as a decomposition–coordination algorithm that combines the separability of dual decomposition with the improved convergence properties of augmented Lagrangian formulations. In particular, it enforces coordination among subproblems through consensus constraints, associated dual variables, and a quadratic penalty term that penalizes mismatches between local and shared boundary variables. This structure enables large problems to be split into smaller subproblems coordinated through iterative local optimization, consensus updates, and dual updates [9]. Owing to its scalability, parallelizability, and limited information exchange requirements, ADMM has been extensively applied to energy system optimization problems.

A substantial body of literature applies ADMM to distributed optimization of electrical power systems, particularly to address scalability limitations of centralized Optimal Power Flow (OPF) formulations. In this context, ADMM is used to decompose large network-constrained OPF problems into regional subproblems while enforcing consistency through boundary-variable consensus. For example, Erseghe [10] proposed an ADMM-based approach for non-convex OPF by partitioning the network into regions and enforcing consensus on shared variables, thereby enabling decentralized computation without convex relaxations. This line of work establishes ADMM as an effective coordination mechanism for large electrical networks; however, it remains focused on operational problems in electricity-only systems.

Beyond transmission-level OPF, ADMM has been widely adopted for distributed energy management in distribution systems and multi-microgrid environments, where coordination among autonomous agents is required. In these settings, ADMM decomposes centralized operational problems into operator- and agent-level subproblems while preserving local autonomy and limiting information exchange. Liu et al. [11] proposed an ADMM-based distributed energy management framework for active distribution networks with networked microgrids, where centralized optimization is decomposed into operator and microgrid-level subproblems coordinated using price-based signals and formulated as MILP problems solvable with standard solvers. Rajaei et al. [12] introduced a transactive energy management framework for multi-microgrid systems using ADMM to coordinate independently operated microgrids using market-like signals. Similarly, Lou and Fujimura [13] addressed distributed energy management of multi-microgrid systems by applying an ADMM-based coordination scheme combined with average-consensus mechanisms, avoiding reliance on global system information. These approaches primarily target short-term operational coordination in electricity distribution systems and do not address integrated multi-energy coupling or design-related decisions.

Several studies extend ADMM-based coordination beyond electricity-only applications to the operational optimization of integrated or multi-energy systems. In this stream, ADMM is used to manage the physical and operational coupling among multiple energy carriers while decomposing the overall problem into locally solvable subproblems. Chen et al. [14] investigated distributed coordination of shared energy storage among multiple park-level integrated energy systems. Zhong et al. [15] studied building-level multi-energy hubs and proposed a distributed auction-based coordination mechanism in which ADMM decomposes the social-welfare optimization across users. Zhu et al. [16] addressed distributed economic dispatch in multi-energy systems with energy storage, considering coordinated operation across electricity, gas, and heat through interconnected energy hubs. Zhou et al. [17] investigated distributed optimal operation of clusters of micro-energy grids within integrated systems including electricity, heat, gas, and hydrogen, using ADMM to coordinate power exchanges among agents. While these works demonstrate the flexibility of ADMM for operational coordination across multiple energy carriers, they remain focused on short-term operation and do not consider network expansion or integrated design-and-operation optimization.

ADMM has been widely applied to the distributed optimization of tightly coupled energy networks. In the operational context, Xu et al. [18] investigated distributed coordination of coupled electricity, heating, and natural gas networks, while Wen et al. [19] developed ADMM-based approaches for the synergistic operation of electricity and natural gas systems under multi-operator architectures. These studies focus primarily on short-term operational coordination and do not address long-term infrastructure investment decisions.

Extending ADMM to planning problems, Yang et al. [20] and Xuan et al. [21] proposed distributed frameworks for integrated electricity and natural gas systems in which investment and operation decisions are optimized simultaneously. Their decomposition strategy is stakeholder-based, partitioning the problem into electricity, gas, and energy-hub operators. In these formulations, each physical network is treated as a single optimization block, and coordination occurs through energy exchanges between stakeholders. Consequently, although the overall problem is distributed across stakeholders, the optimization of each network remains centralized, so that increasing the size or resolution of the network directly increases the complexity of the corresponding subproblem without enabling further structural decomposition. Moreover, thermal energy is modeled at the hub level rather than through an explicitly designed district heating network with capacity sizing and spatially resolved losses.

Overall, while existing ADMM-based approaches demonstrate the effectiveness of distributed coordination for large-scale energy systems, a significant research gap remains. Existing studies mainly address operational coordination or adopt sectoral or stakeholder-based decomposition for integrated electricity–gas planning problems. In these approaches, each physical network is treated as a single optimization block, without spatial-topological decomposition into smaller subdomains. Consequently, increasing network size directly increases the complexity of the corresponding subproblem. Moreover, within this class of applications, the coupling between district heating and electrical networks has received considerably less attention than electricity–gas integrated systems. To the best of the authors' knowledge, no studies have applied spatial-topological decomposition to reduce the computational complexity of combined design and operation optimization problems in MESs that include multiple energy networks.

To address these gaps, building upon the integrated design and operation optimization of MESs, formulated by Dal Cin et al. [5], this work proposes a new ADMM-based distributed optimization framework for large-scale MESs. The goal is to demonstrate that ADMM-based distributed optimization enables an effective simplification of the overall design and operation optimization problem of large-scale MESs, where the computational load is sensibly reduced at the expense of a slight and, therefore, acceptable deterioration of the objective function accuracy. To maintain compatibility with MILP solvers, the augmented Lagrangian penalty term is approximated using a piecewise linear formulation, providing a scalable alternative for the optimization of complex MESs beyond the limits of monolithic approaches.

The novelty of the proposed approach is the introduction of a spatially decomposed ADMM-based framework for integrated design and operation optimization of large-scale MESs, while explicitly capturing the coupling between electrical and thermal infrastructures. This represents an advancement over the existing literature, where sectoral decomposition is typically adopted, leading to a direct increase in computational complexity as the spatial extent of the system and its networks expands.

2. Case Study

In this work, a mixed residential–commercial urban district is considered as the case study. As shown in Figure 1, the system is modeled as a multi-nodal MES consisting of 60 nodes. The nodes represent end users, energy hubs, network junctions, and points of connection with the main electricity grid. Residential and office buildings are distributed throughout the district and are connected to both the electrical microgrid and the District Heating Network (DHN). Each building is characterized by its own electricity and heating demand profiles and is explicitly represented in the network model.

The district is located in Padova, Italy, and comprises 12 residential buildings, 5 office buildings, 4 energy hubs, and 4 connection points with the national electrical grid. Each building is equipped with a Photovoltaic (PV) system and a lithium-ion battery-based Electrical Energy Storage (EES) unit to locally generate and store electricity to meet its demand. The energy hubs, located at nodes 7, 24, 45, and 54, include a gas-fueled combined heat and power Internal Combustion Engine (ICE), a gas boiler, an air–water Heat Pump (HP), and a Thermal Energy Storage (TES) system. These hubs can supply heat to the district heating network, which distributes the required thermal energy to the end users.

To preserve the linearity of the optimization problem, the operating parameters of both the electrical and thermal networks are fixed a priori and assumed constant over the entire operating horizon, as described in [5]. Under this assumption, the networks are modeled by considering only active power flows in the electrical microgrid and heat flows in the DHN. The supply and return temperatures of the DHN are fixed at 70°C and 40°C, respectively, while the electrical microgrid operates at a voltage level of 380 V.

Table 1 reports the annual electricity and heating demands of the end users, together with the corresponding peak demand values observed during the year.

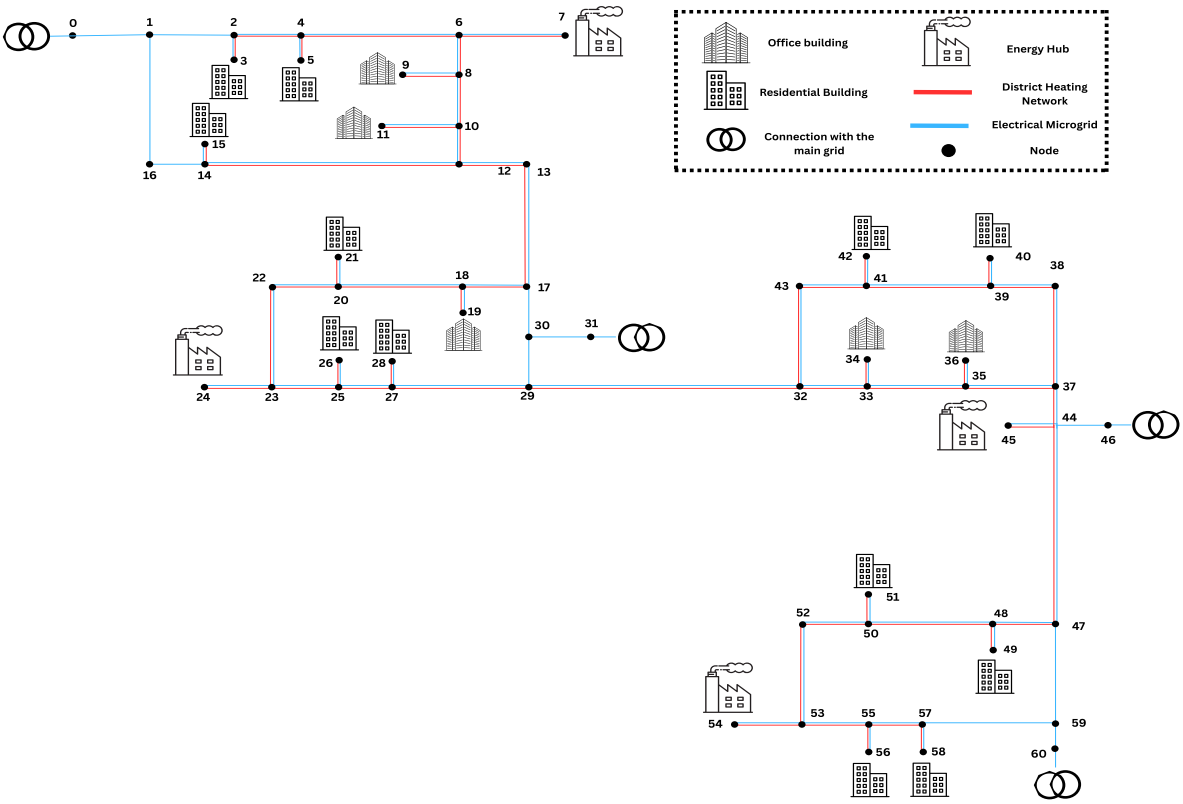

***Figure 1**. Layout of the Case Study*

***Table 1**: Yearly electricity and heating demands ($D_{el,year}$ and $D_{th,year}$, respectively) of each end user and aggregated, with the associated demand peaks over the year ($D_{el,peak}$ for electricity, and $D_{th,peak}$ for heating).*

Node	*3*	*5*	*9*	*11*	*15*	*19*	*21*	*26*	*28*	*34*	*36*	*40*	*42*	*49*	*51*	*56*	*58*	*Aggregated*
$D_{el,year}$ [MWh]	90	126	175	125	144	223	138	179	115	102	183	157	126	239	196	143	121	2582
$D_{th,year}$ [MWh]	73	98	21	17	123	61	108	147	94	12	22	129	103	186	153	111	95	1553
$D_{el,peak}$ [kW]	25	35	70	50	40	79	38	50	32	41	73	44	35	66	54	40	34	682
$D_{th,peak}$ [kW]	60	80	60	50	100	79	88	120	77	35	63	105	84	152	125	91	77	1434

3. Methods

To address the scalability limitations of the monolithic MILP formulation in large-scale districts, the optimization problem is reformulated within a distributed framework based on ADMM. In this work, the term monolithic MILP problem refers to the single, centralized optimization model that represents the entire district as one integrated system and is solved as a single MILP model.

The monolithic MILP is characterized by a single objective function representing the total annualized cost of the MES. This objective includes both operational costs (F_{op}, e.g., fuel consumption and electricity import/export) and investment costs (F_{inv}, e.g., installed capacities of generation units, storage systems, and network branches). It depends simultaneously on operational decision variables, including the power input/output levels and on/off states of dispatchable conversion technologies, storage charging/discharging rates, storage states of charge, power import/export, and network power flows, as well as on design decision variables, such as the installed capacities of technologies and network components.

In compact form, the optimization problem can be expressed as:

$$\min F(x) = F_{\text{op}}(x) + F_{\text{inv}}(x). \tag{1}$$

subject to energy balance equations, network constraints, and technological capacity limits.

Here, x denotes the vector collecting all operational and design decision variables of the system. The detailed mathematical formulation of the monolithic MILP model is provided in [5].

Although this monolithic formulation preserves the full integration of design and operation decisions, the number of continuous and binary variables grows significantly with district size, leading to computational challenges. To improve scalability of the MES, the district is spatially partitioned into multiple interconnected areas. Each area solves a local MILP subproblem, which contains the subset of decision variables and constraints associated with that area. Importantly, the objective of each local MILP subproblem represents only a portion of the global objective function, and the sum of all local objectives is equal to the objective function of the monolithic MILP problem.

The interaction between areas occurs exclusively through boundary flows, i.e., the power and heat flows circulating in electrical lines and district heating pipes that connect nodes belonging to different areas. These boundary flows are the only coupling variables between local MILP subproblems. To ensure physical consistency of the interconnected networks, duplicated local representations of these boundary flows are enforced to be equal across neighboring areas through consensus constraints.

This distributed reformulation preserves the integrated nature of the original design and operation problem while enabling scalable solution through spatial decomposition and parallelizable local computations.

3.1 Spatial Partitioning of the District

First a spatial partition of the district is introduced, resulting in a set of interconnected areas:

$$\mathcal{A} = \{1,2,\dots,\mathrm{A}\}.$$

Each area $a \in \mathcal{A}$ consists of a subset of nodes, which may include residential or office buildings (end users), energy hubs, grid-connection nodes, and portions of the Electrical Distribution Network (EDN) and District Heating Network (DHN). In addition to the internal components of each area, interconnections between areas occur through boundary assets. These include a set of boundary electrical lines, denoted by E_b^{EDN}, representing electrical lines connecting nodes that belong to different areas, and a set of boundary district heating pipes, denoted by H_b^{DHN}, representing thermal pipes connecting nodes located in different areas.

Figures 2.a and 2.b illustrate two examples of spatial partitioning configurations of the district, consisting of two and four interconnected areas, respectively.

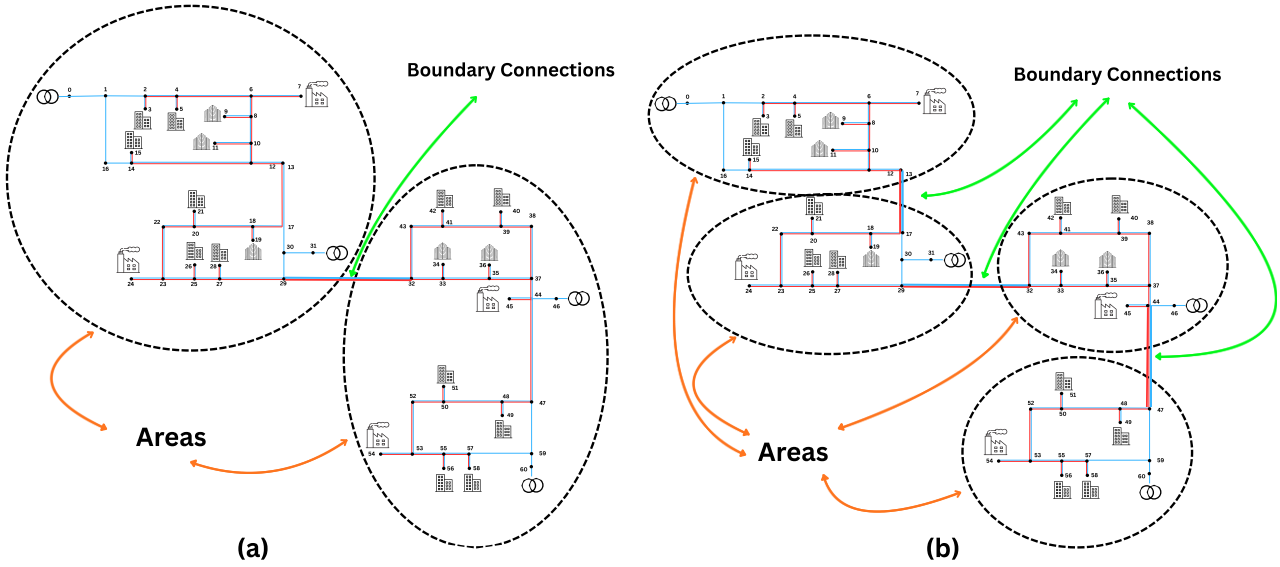

***Figure 2**: Spatial partitioning configurations of the district used in the ADMM framework: a) two-area decomposition and b) four-area decomposition. Dashed contours indicate the spatial areas, while colored links represent boundary connections between areas through electrical and district heating networks.*

3.2 Distributed Problem Formulation in Consensus Form

For each area $a \in \mathcal{A}$, a local optimization problem is defined with the objective of minimizing a local cost function F_a, composed of investment and operational contributions:

$$F_a = F_a^{\mathrm{op}} + F_a^{\mathrm{inv}} \tag{2}$$

where F_a^{op} is the operational cost component and F_a^{inv} is the investment cost component.

The distributed optimization problem can be written in consensus form as:

$$\min_{\{x_a\},\, z} \sum_{a\in\mathcal{A}} F_a\,(x_a) \tag{3}$$

$$x_a \in \mathcal{X}_a, \forall a \in \mathcal{A},$$

$$\text{s.t.} \qquad f_{lkt}^{(a)} = \mathrm{z}_{lkt}, \quad \forall l \in E_b^{\mathrm{EDN}} \cup H_b^{\mathrm{DHN}}, \forall a \in \mathcal{A}_l, \forall k, t,$$

The $f_{lkt}^{(a)}$ denotes the local net boundary flow computed by area $\boldsymbol{a}$ on boundary branch $\boldsymbol{l}$ at representative day $\boldsymbol{k}$ and time step $\boldsymbol{t}$. Depending on the type of branch $\boldsymbol{l}$, this variable represents either electrical power flow (for EDN boundary lines) or heat flow (for DHN boundary pipes). The vector x_a collects all local decision variables of area a, including continuous investment variables (e.g., installed capacities and network sizes), operational variables (dispatch levels, storage states, energy flows), and binary variables (e.g., on/off states of conversion units). The feasible set of area a, denoted by $\mathcal{X}_a$, is the set of all admissible values of the decision vector x_a that satisfy the local physical and operational constraints of area a, including local energy balances, technology limits, storage dynamics, and internal network capacity constraints. Here, $\mathcal{A}$ denotes the set of all areas obtained from the spatial partitioning. For each boundary branch l, the subset $\mathcal{A}_l \subseteq \mathcal{A}$ contains the areas connected by branch l, i.e., the areas that exchange power or heat through that branch.

The variable z_{lkt} is an auxiliary global consensus variable introduced to enforce consistency between the local copies of boundary flows associated with neighboring areas. Physically, it represents the unique energy flow that must be shared by the two areas connected through boundary branch l. For instance, assume that the two areas *a* and *b* are connected through a single branch *l*. Consequently, the previous consistency constraint imposes both $f_{lkt}^{(a)} = \mathrm{z}_{lkt}$ and $f_{lkt}^{(b)} = \mathrm{z}_{lkt}$, so that, as a result, $f_{lkt}^{(a)} = f_{lkt}^{(b)}$. By introducing z_{lkt}, the original coupling between areas is reformulated as equality constraints, allowing the local objective functions to remain separable while avoiding the explicit constraint $f_{lkt}^{(a)} = f_{lkt}^{(b)}$.

3.3 ADMM-Based Solution Procedure

To solve the consensus problem, the augmented Lagrangian is first constructed. In the classical (unscaled) formulation, each consensus constraint $f_{lkt}^{(a)} = \mathrm{z}_{lkt}$ is associated with a Lagrange multiplier $\lambda_{lkt}^{(a)}$, which measures the sensitivity of the objective function to violations of that constraint [22]. The corresponding unscaled augmented Lagrangian is expressed as follows:

$$\mathcal{L}_\rho(\{x_a\}, z, \{\lambda_a\}) = \sum_{a\in\mathcal{A}} F_a\,(x_a) + \sum_{l}\sum_{a\in\mathcal{A}_l}\sum_{k,t} \lambda_{lkt}^{(a)}\big(f_{lkt}^{(a)} - z_{lkt}\big) + \frac{\rho}{2}\sum_{l}\sum_{a\in\mathcal{A}_l}\sum_{k,t}\big(f_{lkt}^{(a)} - z_{lkt}\big)^2. \tag{4}$$

To simplify the notation and improve numerical stability, the scaled dual variable u is introduced and defined as $u_{lkt}^{(a)} = \lambda_{lkt}^{(a)}/\rho$, where ρ is a penalty coefficient. Using this definition, the augmented Lagrangian can be rewritten in the scaled form adopted in this work [9]:

$$\mathcal{L}_\rho(\{x_a\}, z, \{u_a\}) = \sum_{a\in\mathcal{A}} F_a\,(x_a) + \frac{\rho}{2}\sum_{l}\sum_{a\in\mathcal{A}_l}\sum_{k,t}\big(f_{lkt}^{(a)} - z_{lkt} + u_{lkt}^{(a)}\big)^2. \tag{5}$$

The quadratic penalty term (i.e., the second term of the augmented Lagrangian) penalizes mismatches between local boundary flows and the corresponding consensus variable. The penalty coefficient $\rho > 0$ scales this mismatch and influences the convergence behavior of the ADMM iterations.

Since the quadratic penalty term introduces nonlinear expressions into the local subproblems, a Piecewise-Linear (PWL) approximation is employed to preserve the MILP structure of each area problem. The squared residual term is approximated using a set of linear segments, allowing the penalized local problems to remain solvable with standard MILP solvers. This approximation enables the integration of ADMM within the original MILP framework without introducing nonlinear programming complexity [23].

ADMM solves the consensus problem by minimizing the augmented Lagrangian alternately with respect to the local variables x_a and the consensus variables z, followed by an update of the dual variables. The overall workflow of the proposed ADMM algorithm is illustrated in Figure 3.

Let *j* denote the iteration index. In principle, the consensus variables z^0 may be initialized with arbitrary values, for example using a feasible estimate of the boundary flows. In the present work, however, a zero initialization is adopted. The dual variables are also initialized to zero, i.e.,

$$z_{lkt}^0 = 0, \quad u_{lkt}^{(a),0} = 0,$$

for all boundary branches $\boldsymbol{l}$, representative days $\boldsymbol{k}$, time steps $\boldsymbol{t}$, and areas $\boldsymbol{a} \in \boldsymbol{A_l}$.

At iteration $j+1$, the following three steps are performed:

1) Local optimization (x-update):

$$x_a^{j+1} = \arg\min_{x_a \in \mathcal{X}_a} \left\{ F_a(x_a) + \frac{\rho^{j+1}}{2} \sum_l \sum_{k,t} \left(f_{lkt}^{(a)} - z_{lkt}^j + u_{lkt}^{(a),j} \right)^2 \right\}. \tag{6}$$

This step updates investment and operational variables while accounting for disagreement with neighboring areas. Since the augmented terms only involve boundary variables, each area can solve its problem independently. All local MILPs are therefore solved in parallel.

2) Consensus update (z-update):

$$z_{lkt}^{j+1} = \frac{1}{|\mathcal{A}_l|} \sum_{a \in \mathcal{A}_l} \left(f_{lkt}^{(a),j+1} + u_{lkt}^{(a),j} \right). \tag{7}$$

This step enforces agreement among neighboring areas.

3) Dual update (u-update):

$$u_{lkt}^{(a),j+1} = u_{lkt}^{(a),j} + \left(f_{lkt}^{(a),j+1} - z_{lkt}^{j+1} \right). \tag{8}$$

The dual variables accumulate the residual mismatch and guide subsequent iterations toward consensus.

3.3.1 Stopping criteria

The stopping conditions of the ADMM algorithm are defined based on the primal and dual residuals. The residuals are first computed separately for the EDN and the DHN by measuring the deviation between the local boundary flows of each area and the corresponding consensus variables, as well as the change of the consensus variables between successive iterations. The residuals of both networks are then aggregated into global norms, and the algorithm terminates when both the global primal and dual residuals fall below the predefined tolerance. The residuals are defined as follows [9]:

- *Primal residual:* The primal residual measures violation of consensus constraints:

$$r^{j+1} = \left(\sum_l \sum_{a \in \mathcal{A}_l} \sum_{k,t} \left(f_{lkt}^{(a),j+1} - z_{lkt}^{j+1} \right)^2 \right)^{1/2}; \tag{9}$$

- *Dual residual:* The dual residual measures change in consensus variables:

$$s^{j+1} = \left(\sum_l \sum_{k,t} \left(\rho^{j+1} (z_{lkt}^{j+1} - z_{lkt}^j) \right)^2 \right)^{1/2}. \tag{10}$$

The algorithm is terminated when both residuals fall below predefined tolerances or when the maximum number of iterations is reached. In this study, the termination tolerance is set to 10^{-3}.

3.3.2 Adaptive penalty update

To improve convergence robustness and maintain a suitable balance between the primal and dual residuals, the penalty parameters are updated adaptively using a residual-balancing strategy [9]. Before iteration j+1, the penalty parameter is updated based on the residuals computed at iteration j as:

$$\rho^{j+1} = \begin{cases} \tau \rho^j, & \text{if } r^j > \mu s^j, \\ \rho^j / \tau, & \text{if } s^j > \mu r^j, \\ \rho^j, & \text{otherwise,} \end{cases} \tag{11}$$

where $\mu > 1$ and $\tau > 1$ are algorithmic parameters. According to [9] the typical choice might be $\mu = 10$ and $\tau = 2$. In this study, these values are adopted. Thus, the penalty parameter is increased when the primal residual is dominant, decreased when the dual residual is dominant, and left unchanged when both residuals are of comparable magnitude.

Since the scaled dual variable satisfies $u = \lambda / \rho$, any update of the penalty parameter requires a rescaling of the dual variable to keep the unscaled multiplier unchanged. Therefore, after updating ρ, the scaled dual variable is rescaled as:

$$u^j \leftarrow \frac{\rho^j}{\rho^{j+1}} u^j \tag{12}$$

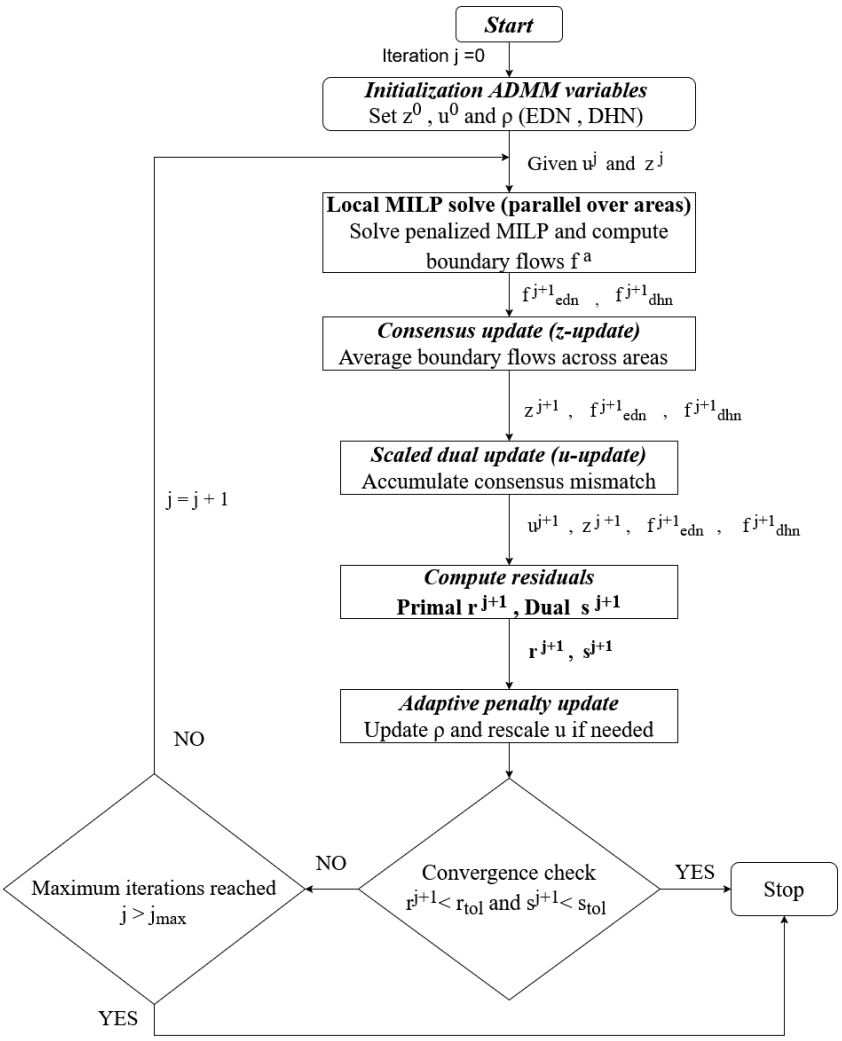

***Figure 3**: Flowchart of ADMM algorithm*

4. Results

Both the monolithic MILP formulation and the proposed ADMM-based distributed formulation are implemented in Python and solved using Gurobi as the MILP optimizer. For all simulations, the relative mixed-integer optimality gap (MIP gap) is set to 2%. The MIP gap represents the relative difference between the best incumbent solution and the best bound provided by the solver and therefore defines the termination tolerance used by the MILP solver. All computations are performed on a workstation equipped with an Intel® Core™ i7-6500U processor (2.50 GHz), 8 GB of RAM, and a 64-bit operating system.

4.1 Reference Solution: Monolithic MILP Formulation

As a benchmark for evaluating the proposed distributed framework, the simultaneous design and operation optimization problem of the case study is first solved using the monolithic MILP formulation. In this configuration, the entire district is modeled and optimized as a single centralized problem without spatial decomposition. The resulting objective value (total annualized life-cycle cost) obtained from the monolithic formulation is used as the reference for assessing the objective accuracy of the distributed ADMM approach.

The monolithic optimization yields a total annualized life-cycle cost of 662.7 k€, consisting of 302.4 k€ in operational costs and 360.3 k€ in investment costs. Compared to the baseline scenario, in which the aggregated electricity demand is fully supplied by the national grid and the aggregated heating demand is met exclusively by natural gas boilers, the optimized solution achieves a 9.2% reduction in total cost (reference value: 730.2 k€).

From an environmental perspective, total annual CO_2 emissions decrease from 1259.2 tCO_2/year in the reference case to 678 tCO_2/year, corresponding to a 46.2% reduction.

Regarding electricity exchange with the main grid, the optimized system imports 356.0 MWh/year and exports 642.6 MWh/year. The resulting electricity self-consumption share reaches 86.2%, while approximately 21% of locally generated electricity is exported to the grid. The installed capacities of the technologies obtained from

the optimization are also summarized in Table 2, where the total installed capacity corresponds to the sum of the capacities installed across all nodes of the district.

The monolithic MILP contains 87,447 continuous variables and 1920 binary variables. Solving this centralized optimization problem requires 16,935 seconds (approximately 4.7 hours) to reach the prescribed optimality tolerance of 2%.

4.2 ADMM-Based Distributed Optimization

To evaluate the performance of the proposed distributed optimization framework, the case study is solved using ADMM under two spatial partitioning strategies: a two-area decomposition and a four-area decomposition. In both cases, the district energy system is divided into interconnected areas that exchange both electricity and heat through boundary electrical lines and heating network pipes.

The results obtained with the ADMM algorithm are mainly compared with the monolithic benchmark in terms of (i) computational time and (ii) deviation of the objective function value from the monolithic benchmark.

Table 2 summarizes the key quantities and performance indicators obtained with the monolithic formulation and the two distributed ADMM configurations.

***Table 2**: Comparison between monolithic MILP and ADMM-based distributed solutions*

Indicator	Monolithic MILP	ADMM (2 areas)	ADMM (4 areas)
Objective value [k€]	662.7	664.0 (+0.19%)	673.6 (+1.6%)
Investment cost [k€]	360.3	367.8 (+2.1%)	391.5 (+8.7%)
Operational cost [k€]	302.4	296.2 (-2.05%)	282.0 (-6.7%)
Annual CO_2 emissions [tCO_2/y]	678	669.8 (-1.2%)	660 (-2.7%)
Electricity import [MWh/y]	356.0	346.9 (-2.5%)	317.4 (-10.8%)
Electricity export [MWh/y]	642.6	672.1 (+4.6%)	777.3 (+20.9%)
Electricity self-consumption [%]	86.2	78.3 (-9.2%)	76 (-11.8%)
PV [kW_p]	1349.8	1381.6 (+2.3%)	1495.5 (+10.8%)
ICE [kW_{el}]	318.5	325.6 (+2.2%)	282.8 (-11%)
Gas boiler [kW_{th}]	621.8	581 (-6.6%)	612.1 (-1.5%)
Heat Pump [kW_{th}]	417.7	423.1 (+1.3%)	422.2 (+1.1%)
Hot Water Tank [kWh]	255.5	351.9 (+37.7%)	453.8 (+77.6%)
Lithium battery [kWh]	423.5	473.4 (+11.8%)	600.3 (+41.7%)
Computational time [s]	16,935	12,000 (-29%)	5,800 (-65.7%)
Maximum binary variables in a subproblem	1920	960 (-50%)	480 (-75%)
Maximum continuous variables in a subproblem	87447	46925 (-46%)	26266 (-70%)
ADMM iterations	–	8	9

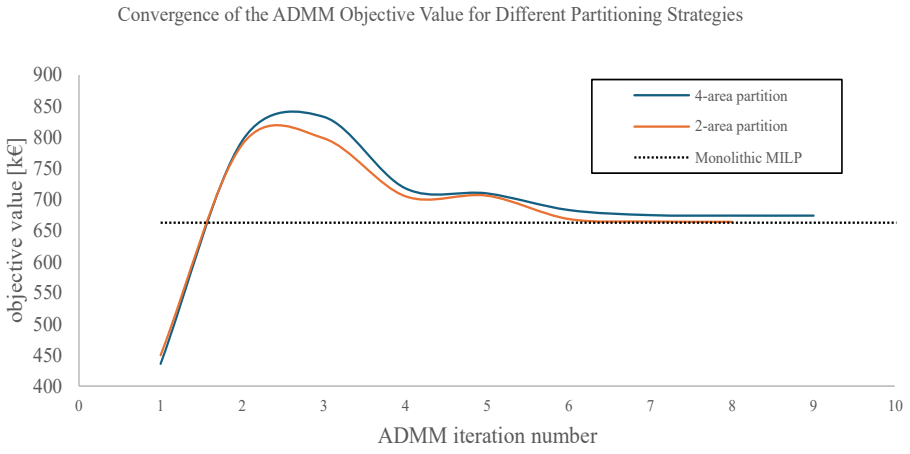

Figure 4: Convergence of the ADMM objective value over iterations for the two-area and four-area decompositions compared with the monolithic MILP benchmark.

The convergence behavior of the ADMM algorithm is illustrated in Figure 4, which shows the evolution of the objective function value across iterations for both the two-area and four-area partitioning strategies. In both cases, the distributed solution progressively approaches the objective value obtained with the monolithic MILP benchmark, confirming the convergence of the distributed coordination process.

4.2.1 Four-area decomposition

In the first scenario, the district is decomposed into four interconnected areas, as illustrated in Figure 2b. For this configuration, the ADMM-based distributed approach yields a total annualized life-cycle cost of 673.6 k€, consisting of 282.0 k€ in operational costs and 391.5 k€ in investment costs. These values are obtained by aggregating the results of the individual areas, meaning that the overall objective value corresponds to the sum of the investment and operational costs computed in the local MILP subproblems.

Compared with the monolithic MILP benchmark (662.7 k€), the distributed solution shows an objective value deviation of approximately 1.6%. This difference is expected, since ADMM applied to mixed-integer optimization problems does not generally guarantee convergence to the global optimum. Nevertheless, the deviation remains limited, confirming that the distributed formulation can provide near-optimal solutions. A closer inspection of Table 2 reveals that the largest deviations are concentrated in electricity import/export and in the capacities of storage technologies. In particular, the four-area decomposition leads to higher installed capacities of lithium batteries (+41.7%) and hot water tanks (+77.6%), together with a moderate increase in PV capacity (+10.8%) and a decrease in ICE capacity (−11%). This pattern can be explained by the fact that each area is solved as a separate local optimization problem with only partial knowledge of the global system, and tends to rely on its own flexibility resources, as coordination across areas is achieved only through boundary-flow consensus constraints. The increase in PV and storage capacities allows a larger share of the demand to be balanced locally and reduces electricity imports from the main grid (-10.8%). At the same time, since the increase in local renewable generation exceeds the additional storage absorption capacity, surplus electricity exported to the grid also increases (+20.9%). Therefore, the distributed solution achieves lower operating costs (-6.7%), but at the expense of higher investment costs (+8.7%), which explains the overall increase in the total annualized cost.

From an environmental perspective, total annual CO_2 emissions amount to 660 tCO_2/year, which is slightly lower than the value obtained with the monolithic formulation (678 tCO_2/year), indicating that the distributed solution preserves comparable environmental performance. This reduction is consistent with the higher penetration of PV generation and the lower dependence on grid electricity imports.

From a computational perspective, the distributed formulation significantly reduces the solution time. While the centralized MILP requires 16,935 seconds, the ADMM algorithm converges in approximately 5,800 seconds, corresponding to a reduction of about 65% in computational time. Convergence is achieved after 9 ADMM iterations, and the evolution of the objective function value over the ADMM iterations is illustrated in Figure 4. The reduction in computational time is primarily due to the smaller size of the local optimization problems, which can be solved independently and in parallel. In the distributed formulation, each area contains 480 binary variables, while the number of continuous variables in Areas 1–4 is 25,463, 25,304, 26,266, and 22,380 respectively. This represents a substantial reduction in problem size compared to the centralized MILP.

4.2.2 Two-area decomposition

To further investigate the impact of spatial partitioning, the case study is also solved using a two-area decomposition as illustrated in Figure 2a. In this scenario, the ADMM-based approach yields an objective value of 664.0 k€, which is very close to the monolithic benchmark (+0.19%). The corresponding computational time is approximately 12,000 seconds (3.3 hours), representing a reduction of about 29% compared to the monolithic formulation. In this configuration, each area contains 960 binary variables, while the numbers of continuous variables are 46,925 and 44,364 for Areas 1 and 2 respectively. Convergence is achieved after 8 ADMM iterations, as also illustrated by the convergence trend reported in Figure 4.

As shown in Table 2, the two-area decomposition produces results that remain very close to the centralized solution across most performance indicators. The investment cost increases by only 2.1% compared to the monolithic case, while the operational cost decreases slightly by 2.1%. Similarly, environmental performance remains close to the centralized benchmark. Annual CO_2 emissions decrease by approximately 1.2% relative to the monolithic case.

The same trend is observed for electricity exchange indicators. Electricity imports decrease by 2.5%, while electricity exports increase by 4.6%. The electricity self-consumption rate decreases moderately to 78.3%, which remains closer to the centralized solution than in the four-area case.

Installed capacities of technologies also show relatively small deviations from the centralized solution, with most remaining below 10%. For instance, the photovoltaic capacity increases by only 2.3%, while the internal combustion engine capacity increases slightly by 2.2%. The largest deviation is observed for the hot water tank capacity, which increases by 37.7%. Consistent with the rationale discussed in Section 4.2.1, the two-area decomposition shows qualitatively similar but smaller deviations in storage capacities and electricity exchange, since the lower number of boundary cuts preserves a greater degree of global coordination.

5. Conclusions

This work addresses the scalability limitations of the integrated design and operation optimization of large-scale Multi-Energy Systems (MESs). Starting from the monolithic Mixed Integer Linear Programming (MILP) formulation commonly used for district-scale MES optimization, a distributed optimization framework based on the Alternating Direction Method of Multipliers (ADMM) is presented. The proposed approach reformulates the centralized problem into spatially decomposed local MILP subproblems, which are coordinated through consensus constraints representing electricity and heat exchanges between interconnected areas.

The proposed framework is evaluated on a multi-nodal district energy system including electricity and district heating networks. The results are compared with the centralized monolithic MILP formulation in terms of objective value accuracy and computational time. The centralized optimization yields a total annualized life-cycle cost of 662.7 k€, which serves as the benchmark solution.

The distributed ADMM framework has demonstrated its capability to significantly reduce computational time while maintaining near-optimal solution quality. In the two-area decomposition scenario, the distributed solution achieves an objective value of 664.0 k€, corresponding to a deviation of only 0.19% from the centralized benchmark, while reducing computational time by approximately 29%. In the four-area decomposition, the computational time is reduced by about 65%, while the objective deviation is 1.6%.

The results further highlight the influence of the spatial partitioning strategy on the performance of the distributed optimization. Increasing the number of areas reduces the size of the local MILP subproblems and enables faster parallel computation. However, a finer partition also increases the number of boundary connections between areas, which introduces stronger coupling constraints that must be coordinated through the ADMM iterations. Consequently, while a higher number of areas leads to greater computational acceleration, it may also result in slightly larger deviations from the centralized optimal solution.

Overall, the proposed ADMM-based distributed framework provides a scalable solution approach for integrated design and operation optimization of large-scale multi-energy systems. By enabling spatial decomposition while preserving the integrated nature of the optimization problem, the method significantly improves computational tractability while maintaining high solution accuracy. These results demonstrate the potential of the proposed framework to extend detailed MES optimization models to larger geographical systems, such as city-scale energy networks.

Acknowledgments

Project financially supported by BIRD 2024 Research Program of University of Padova (2024DII1SIDPROGETTI-00252).

Nomenclature

Abbreviations

ADMM	Alternating Direction Method of Multipliers
MES	Multi-Energy System
MILP	Mixed-Integer Linear Programming
SDO	Synthesis–Design–Operation optimization
EDN	Electrical Distribution Network
DHN	District Heating Network
PV	Photovoltaic
EES	Electrical Energy Storage
TES	Thermal Energy Storage
ICE	Internal Combustion Engine
HP	Heat Pump
OPF	Optimal Power Flow

Sets and indices

$\mathcal{A}$	Set of areas (spatial subdomains) in the district.
$\mathcal{A}_l$	subset of areas connected to branch l
a	Index of area, $a \in \mathcal{A}$
l	Index of boundary branch (electrical line or heating pipe).
k	Index of representative day.
t	Index of time step within a representative day.

References

[1] European Commission (EC), "Communication from the Commission to the European Parliament and the Council: EU-wide assessment of the final updated national energy and climate plans – Delivering the Union's 2030 energy and climate objectives," European Commission , Brussels, 2025.

[2] Tim Felling, Oliver Levers, Philipp Fortenbacher, "Multi-horizon planning of multi-energy systems," Electric Power Systems Research, vol. 212, 2022.

[3] Gabriele Volpato, Gianluca Carraro, Marco Cont, Piero Danieli, Sergio Rech, Andrea Lazzaretto, "General guidelines for the optimal economic aggregation of prosumers in energy communities," Energy, vol. 258, 2022.

[4] C. A. Frangopoulos, "Recent developments and trends in optimization of energy systems," Energy, vol. 164, pp. 1011-1020, 2018.

[5] Enrico Dal Cin, Gianluca Carraro, Gabriele Volpato, Andrea Lazzaretto, George Tsatsaronis, "DOMES: A general optimization method for the integrated design of energy conversion, storage and networks in multi-energy systems," Applied Energy, vol. 377, 2025.

[6] Leander Kotzur, Lars Nolting, Maximilian Hoffmann, Theresa Groß, Andreas Smolenko, Jan Priesmann, Henrik Büsing, Robin Beer, Felix Kullmann, Bismark Singh, Aaron Praktiknjo, Detlef Stolten, Martin Robinius, "A modeler's guide to handle complexity in energy systems optimization," Advances in Applied Energy, vol. 4, 2021.

[7] Conejo Antonio J.,Castillo Enrique,Mínguez Roberto,García-Bertrand Raquel, Decomposition techniques in mathematical programming: Engineering and science applications, 2006.

[8] C. Sagastizábal, "Divide to conquer: decomposition methods for energy optimization," Math. Program, vol. 134, pp. 187-222, 2012.

[9] Boyd, Stephen & Parikh, Neal & Chu, Eric & Peleato, Borja & Eckstein, Jonathan, "Distributed Optimization and Statistical Learning via the Alternating Direction Method of Multipliers," Foundations and Trends in Machine Learning, vol. 3, pp. 1-122, 2011.

[10] T. Erseghe, "A distributed approach to the OPF problem," EURASIP Journal on Advances in Signal Processing, vol. 45, 2015.

[11] Guodong Liu, Maximiliano F. Ferrari, Yang Chen, "A Mixed integer linear programming-based distributed energy management for networked microgrids considering network operational objectives and constraints," IET Energy Systems Integration, 2023.

[12] Ali Rajaei, Sajjad Fattaheian-Dehkordi, Mahmud Fotuhi-Firuzabad, Moein Moeini-Aghtaie, "Decentralized transactive energy management of multi-microgrid distribution systems based on ADMM," International Journal of Electrical Power & Energy Systems, vol. 132, 2021.

[13] Huen Lou, Shigeru Fujimura, "ADMM-Based Distributed Algorithm for Energy Management in Multi-Microgrid System," IEEJ Transactions on Electrical and Electronic Engineering, vol. 19, 2024.

[14] Jianfei Chen, Ke Li, Haiyang Wang, Daduan Zhao, Chao Jiang, Chenghui Zhang, "Distributed parallel optimal operation for shared energy storage system - multiple park integrated energy system based on ADMM," Energy, vol. 317, 2025.

[15] W. Zhong, C. Yang, K. Xie, S. Xie and Y. Zhang, "ADMM-Based Distributed Auction Mechanism for Energy Hub Scheduling in Smart Buildings," IEEE Access, vol. 6, pp. 45635-45645, 2018.

[16] S. Zhu, T. Ding, C. Chen, M. -Y. Chow and X. Guan, "DEED-ADMM: A Scalable Distributed Algorithm for Economic Dispatch in Multi-Energy Systems With Energy Storage," IEEE Transactions on Automation Science and Engineering, vol. 22, pp. 11431-11443, 2025.

[17] Zhou Dongxu , Xu Jingzhou , Zhang Can , Wei Pengchao , Pan Guangsheng , Gu Zhongfan, "A multi-agent optimal operation methodology of electric, thermal, and hydrogen integrated energy system based on ADMM algorithm," Frontiers in Energy Research, p. 12, 2024.

[18] Da Xu, Qiuwei Wu, Bin Zhou, Canbing Li, Li Bai, Sheng Huang, "Distributed Multi-Energy Operation of Coupled Electricity, Heating, and Natural Gas Networks," IEEE Transactions on Sustainable Energy, vol. 11, 2020.

[19] Yunfeng Wen, Xiaobin Qu, Wenyuan Li, Xuan Liu, Xi Ye, "Synergistic Operation of Electricity and Natural Gas Networks via ADMM," IEEE Transactions on Smart Grid, vol. 9, 2018.

[20] Hangbo Yang, Pengcheng You, Ce Shang, "Distributed planning of electricity and natural gas networks and energy hubs," Applied Energy, vol. 282, 2021.

[21] Ang Xuan, Yingfei Sun, Zhengguang Liu, Peijun Zheng, Weike Peng, "An ADMM-based tripartite distributed planning approach in integrated electricity and natural gas system," Applied Energy, 2025.

[22] Jorge Nocedal , Stephen J. Wright, Numerical Optimization, Springer, 2006.

[23] Guodong Liu; Maximiliano Ferrari; Yang Chen, "A Mixed Integer Linear Programming-based Distributed Energy Management for Three-phase Unbalanced Active Distribution Network," IEEE Kansas Power and Energy Conference (KPEC), 2024.